Chemical Science

ROYAL SOCIETY OF CHEMISTRY

EDGE ARTICLE

View Article Online
View Journal | View Issue



Cite this: *Chem. Sci.*, 2021, **12**, 12315

All publication charges for this article have been paid for by the Royal Society of Chemistry

Received 15th July 2021
Accepted 29th July 2021

DOI: 10.1039/d1sc03856g

rsc.li/chemical-science



# Mg(II) heterodinuclear catalysts delivering carbon dioxide derived multi-block polymers†

Gloria Rosetto, Arron C. Deacy and Charlotte K. Williams *

Carbon dioxide derived polymers are emerging as useful materials for applications spanning packaging, construction, house-hold goods and automotive components. To accelerate and broaden their uptake requires both more active and selective catalysts and greater structural diversity for the carbon dioxide derived polymers. Here, highly active catalysts show controllable selectivity for the enchainment of mixtures of epoxide, anhydride, carbon dioxide and lactone. Firstly, metal dependent selectivity differences are uncovered using a series of dinuclear catalysts, Mg(II)Mg(II), Zn(II)Zn(II), Mg(II)Zn(II), and Mg(II)Co(II), each exposed to mixtures of bio-derived tricyclic anhydride, cyclohexene oxide and carbon dioxide (1 bar). Depending upon the metal combinations, different block structures are possible with Zn(II)Zn(II) yielding poly(ester-*b*-carbonate); Mg(II)Mg(II) or Mg(II)Co(II) catalysts delivering poly(carbonate-*b*-ester); and Mg(II)Zn(II) furnishing a random copolymer. These results indicate that carbon dioxide insertion reactions follow the order Co(II) > Mg(II) > Zn(II). Using the most active and selective catalyst, Mg(II)Co(II), and exploiting reversible on/off switches between carbon dioxide/nitrogen at 1 bar delivers precision triblock (ABA), pentablock (BABAB) and heptablock (ABABABA) polymers (where A = poly(cyclohexylene oxide-*alt*-tricyclic anhydride), PE; B = poly(cyclohexene carbonate), PCHC). The Mg(II)Co(II) catalyst also selectively polymerizes a mixture of anhydride, carbon dioxide, cyclohexene oxide and ε-caprolactone to deliver a CBABC pentablock copolymer (A = PE, B = PCHC C = poly(caprolactone), PCL). The catalysts combine high activity and selectivity to deliver new polymers featuring regularly placed carbon dioxide and biomass derived linkages.

## Introduction

Carbon dioxide/epoxide copolymerization is a front-runner carbon dioxide utilization technology as it is truly catalytic, results in 20–50 wt% carbon dioxide uptake into the polymer backbone and significantly reduces the greenhouse gas emissions associated with polymer production.[1–3] Further attractions include the widespread commercial availability and low-cost of epoxides, processes compatible with existing manufacturing infrastructure and polymers with properties suitable for applications spanning packaging, agricultural films, home-insulation materials, adhesives, coatings, flex-foams for furniture, clothing and automotive components, amongst others.[4] To accelerate and broaden applications requires a greater diversity of carbon dioxide-containing materials and delivering these necessitates advances in the polymerization catalysis.[5,6] One possibility is to copolymerize mixtures of carbon dioxide alongside other monomers so as to 'place' carbonate linkages selectively within more complex copolymer structures.[7,8] More generally, devising atom economical and high yielding methods to control the sequences of both individual monomers and blocks in the polymer backbone is a major challenge.[9,10]

In terms of controlling sequences within alternating polyesters, Coates and co-workers pioneered high activity Al(III) catalysts for epoxide/anhydride ring-opening copolymerization (ROCOP) and applied elegant post-functionalization reactions to install alternating sequences of imine and alkyl group substituents.[11] Subsequently, we also exploited the high alternation of epoxide/anhydride ROCOP to install alternating but orthogonal functional groups producing amphiphilic polymers which self-assembled in aqueous solution.[12] Wu and co-workers prepared self-healable thermoplastic elastomers from $CO_2$/epoxide derived polycarbonates, with precision placement of dynamic cross-linking moieties to the side-chains.[13] These materials showed a Young's modulus of 10 MPa and excellent elastic recovery. Meng and co-workers polymerized mixtures of propylene oxide (PO), cyclohexene oxide (CHO), phthalic anhydride (PA) and $CO_2$ to form polymers with variable ester : carbonate linkages.[14] The materials showed high tensile strength (54 MPa), optical transparency and molar masses up to 70 kg $mol^{-1}$: properties were competitive with polystyrene. Herein, efficient and one-pot polymerization catalyses afford both highly alternating monomer sequences within the blocks and

*Department of Chemistry, Chemistry Research Laboratory, 12 Mansfield Rd, Oxford, OX1 3TA, UK. E-mail: charlotte.williams@chem.ox.ac.uk*

† Electronic supplementary information (ESI) available. See DOI: 10.1039/d1sc03856g

highly selective block sequences within the polymer chain. Catalysts that selectively enchain monomer mixtures to provide specific and single block polymer structures are important targets.[15–17]

In particular, being able to switch catalysts between different mechanisms is useful to diversify the block chemistries.[16,18,19] In 2008, Coates and co-workers described the first example with a Zn(II) catalyst polymerizing a mixture of diglycolic anhydride (DGA), CHO and $CO_2$ to produce a poly(ester-*b*-carbonate).[20] The order of block enchainment was rationalized by >2000-fold faster rate for DGA *vs.* $CO_2$ insertion into the propagating zinc alkoxide intermediate. Subsequently, many other equivalently selective and controlled homogenous mono-,[21–24] dinuclear metal catalysts[25,26] and organocatalysts were reported.[27,28] A few catalysts are exceptions to the selectivity preference, including poorly defined heterogeneous catalysts that result in ill-controlled random or tapered copolymers.[29–31]

In 2014, we reported a new type of self-switchable polymerization catalysis, whereby a Zn(II)Zn(II) catalyst was directed between epoxide/carbon dioxide ROCOP and lactone ring-opening polymerization (ROP) to deliver well controlled poly(ester-*b*-carbonates).[32,33] A year later, the same selectivity and block structures were observed when mixtures of epoxide, anhydride and lactone were polymerized by the di-Zn(II) catalyst.[34] In 2016, a combined experimental and theoretical investigation revealed the 'rules' of switchable catalysis and allowed for the prediction of polymer structures from mixtures of epoxide, carbon dioxide, lactone and anhydride (Fig. 1).[35] It was found that the energy barrier to $CO_2$ insertion into the zinc-alkoxide intermediate was slightly lower than that for anhydride insertion (12.8 kcal $mol^{-1}$ and 16 kcal $mol^{-1}$ respectively), yet experimentally the polyester block formed before the polycarbonate (Fig. 1b). The zinc-carboxylate intermediate is significantly more stable than the corresponding zinc-carbonate and $CO_2$ insertion would be expected to be reversible under the polymerization conditions. Thus, the carboxylate linkage provides a thermodynamic 'sink' driving the selective formation of poly(ester). Subsequently, a range of other metallic, organometallic and organo-catalysts were established to follow the same monomer sequence selectivity 'rules' and the switchable catalysis was shown to apply to different epoxides, anhydrides, lactones and heterocycles.[15,28,36–42]

Despite the successes of switchable catalysis, almost all prior research has focussed on polyesters and -ethers, with a paucity of investigations of carbon dioxide linkage placement.[26,43–47] This likely arises from the limited range of carbon dioxide/epoxide ROCOP catalysts and technical complexities in controlling the gas atmosphere since many catalysts require high pressures and use of stainless-steel reactors. Thus, there remain several notable absences from the emerging field of multi-block polymers produced by switchable catalysis. These include a lack of reports of multiple switching between epoxide/anhydride and carbon dioxide copolymerization to build up multi-block poly(ester-*b*-carbonate) structures and only one prior report of a CBABC pentablock structure combining blocks derived by lactone ROP and epoxide/anhydride/carbon dioxide ROCOP.[48] It's also important to improve the activity of these switchable polymerization catalysts since current best-in-class catalysts fail to perform across multiple polymerization cycles, with turn-over-frequency values limited to 100 $h^{-1}$ at 1 bar of $CO_2$.[25–27]

## Results

It was previously noted that the Zn(II)Zn(II) catalyst **1** exposed to a mixture of cyclohexene oxide, sterically hindered tricyclic anhydride (a bio-based monomer[49,50]) and carbon dioxide resulted in first anhydride and then carbon dioxide insertion forming a poly(ester-*b*-carbonate).[26] Curiously, the analogous Mg(II)Mg(II) catalyst **2** showed the reverse order of insertion resulting in the formation of poly(carbonate-*b*-ester) – a unique selectivity (Fig. 1c).[26] Overall, catalyst **2** is 17 times faster than **1**, however, its activity remains low with a TOF = 77 $h^{-1}$ ([**2**] : [TCA] : [CHO] = 1 : 100 : 1000, 1 bar $CO_2$, 100 °C). The unexpected selectivity difference between Zn(II) and Mg(II) based catalysts motivated further investigation. Two recently

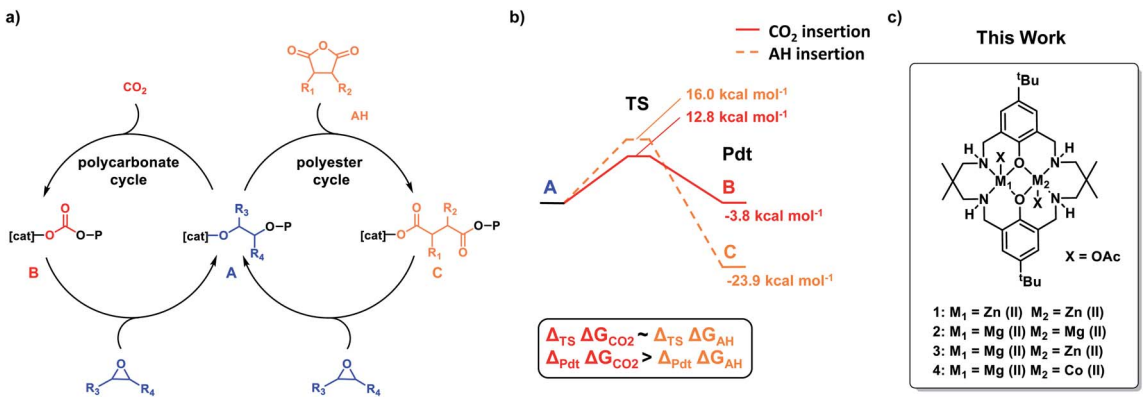


Fig. 1 (a) Catalytic cycles for $CO_2$/epoxide and anhydride (AH)/epoxide ROCOP, connected *via* the catalyst-alkoxide intermediate, A. (b) DFT calculated barriers to the selectivity limiting step to form products (Pdt), comparing carbon dioxide or anhydride insertion into the zinc alkoxide intermediate (A) (calculations were conducted using di-Zn(II) catalyst **1**, cyclohexene oxide CHO, and phthalic anhydride PA). (c) Structures of the dinuclear catalysts **1**–**4** featured in this work.

reported heterodinuclear catalysts, Mg(II)Zn(II) (**3**) and Mg(II)Co(II) (**4**), show higher rates in anhydride/epoxide and $CO_2$/epoxide ROCOP compared with their homodinuclear analogues (Fig. 1c).[51,52] Both catalysts are synergic and in both cases the rate limiting step involves metal coordinated epoxide being attacked by a carbonate/carboxylate nucleophile. This means that the selectivity limiting step, *i.e.* carbon dioxide/anhydride insertion, is pre-rate limiting and as such there's no obvious way to predict selectivity from mixtures of carbon dioxide and anhydride but terpolymerization investigations are expected to reveal it.

Each catalyst was exposed to a mixture of 100 equiv. tricyclic anhydride, TCA, neat cyclohexene oxide (~2000 equiv.), 10 equiv. 1,2-cyclohexenediol (CHD), and 1 bar carbon dioxide pressure, at 100 °C (Scheme 1a). The diol, CHD, functions as a chain transfer agent and results in the formation of α,ω-hydroxyl-telechelic polymers (Fig. S1†).[3] The reactions were monitored using *in situ* IR spectroscopy by measuring the change in absorption intensity of characteristic anhydride (1780 $cm^{-1}$) and polycarbonate (1230 $cm^{-1}$) resonances against time. Catalyst **1** showed selective anhydride consumption and formation of poly(TCA-*alt*-CHO) (Fig. S5 and S6†), hereafter shortened to the abbreviation PE (Table 1). In contrast, catalyst **2** showed selective poly(cyclohexene carbonate), PCHC, formation without any PE (Fig. S7 and S8†) (Table 1, entries 1 and 2). Catalyst **3** (Zn(II)Mg(II)) showed the simultaneous formation of both PE and PCHC linkages in an approximate ratio 1 : 3 (PE : PCHC) by aliquot analysis using $^1$H NMR spectroscopy (Fig. S9†), indicative of faster carbon dioxide than anhydride consumption (Table 1, entry 3). The composition of the crude and purified polymer remained unchanged, as determined by $^1$H NMR spectroscopy, supporting the formation of a random copolymer, *i.e.* poly(carbonate-*r*-ester), rather than mixtures of different polymers (Fig. S10†). The polymer showed a single diffusion coefficient for all signals by DOSY NMR spectroscopy which, again, is indicative of copolymer formation rather than mixtures of PE and PCHC (Fig. S11†). New signals for the carbonyl resonances were observed in the $^{13}C\{^1H\}$ NMR spectrum (Fig. S12†). Catalyst **4** (Mg(II)Co(II)) showed equivalent selectivity to **2** and formed only polycarbonate without any polyester (Fig. S13 and S14†). Its activity was ~6 times greater than **2**, consistent with the previously observed synergy between Co(II) and Mg(II) centres ($TOF_{MgMg} = 112\ h^{-1}$ *vs.* $TOF_{MgCo} = 640\ h^{-1}$, Table 1). All the catalysts showed well controlled polymerizations ($Đ$ <1.2) and produced polyols.

To understand better the differences in catalyst selectivity, the sterically hindered tricyclic anhydride was replaced with lower steric hindrance phthalic anhydride (PA, a commercial monomer used at scale in polymer production). Using either catalyst **1** or **3** resulted in faster anhydride insertion and formation of polyester, *i.e.* PA > $CO_2$ (Table 1, entries 5 and 7) (Fig. S15–S17†). However, using 1 bar pressure of $CO_2$ with either **2** or **4**, formed a random copolymer with ~1 : 4 (PE′ : PC) ester : carbonate linkages implying $CO_2$ > PA (Table 1, entry 6 and 8). In these cases, the aliquots taken throughout the polymerization showed consistent ratios indicating the random ester linkages were distributed within the polymer backbone (Fig. S18†). Characteristic peaks for poly(PA-*alt*-CHO) or PE′ (5.13 ppm), PCHC (4.61 ppm) and junction units (4.98 and 4.47 ppm) were observed in the $^1$H NMR spectrum (Fig. S18 and S19†). *In situ* IR spectroscopic analysis also showed the continual evolution of the carbonate (1230 $cm^{-1}$) resonance and PA consumption (1779 $cm^{-1}$) (Fig. S20†). Further, consistent uptake of carbon dioxide was observed throughout the reaction (Fig. S21†). Thus, both monomers, *i.e.* PA and $CO_2$, are consumed throughout the polymerization but carbon dioxide uptake is faster. The resulting random copolymer shows a $^{13}C\{^1H\}$ NMR spectrum with carbonyl resonances (~154 ppm) at signals distinct from either PE′ or PCHC, once again indicative of random ester enchainment (Fig. S22†). DOSY NMR analysis, of the purified polymer, displays a single diffusion coefficient consistent with all monomers being enchained in a single

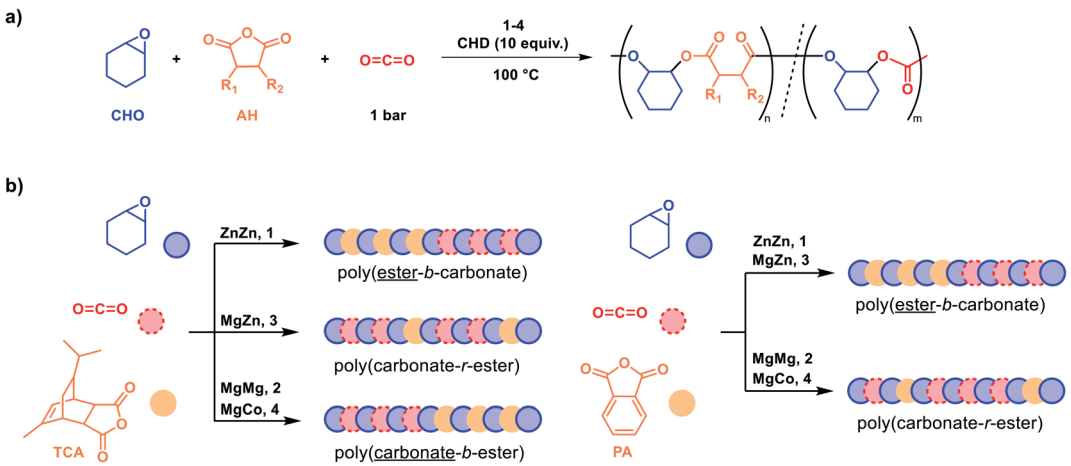


Scheme 1 (a) Schematic showing the synthesis of different copolymers from mixtures of cyclohexene oxide (CHO), anhydride (AH), and $CO_2$, with catalysts **1**–**4**. (b) Summary of catalyst selectivity and the resulting polymer architectures. Note that changing from $CO_2$ to $N_2$ atmosphere is required when using catalysts **2** and **4** to ensure ester formation.

Table 1 Catalyst selectivity data for polymerizations of mixtures of anhydride/CHO/$CO_2$[a]

| | | | | TON[b] | | TOF ($h^{-1}$)[c] | | Composition (%) | | |
|---|---|---|---|---|---|---|---|---|---|---|
| Entry | AH | Catalyst | Time (h) | AH | CHO | PE | PCHC | PE | PCHC | $M_n$ (kg $mol^{-1}$) [$Đ$][d] |
| 1 | TCA | **1** | 7.7 | 82 | 82 | 11 | 0 | 100 | 0 | 1.7 [1.16] |
| 2 | | **2** | 1.5 | 0 | 168 | 0 | 112 | 0 | 100 | 2.3 [1.15] |
| 3 | | **3** | 1.5 | 100 | 407 | 67 | 205 | 25 | 75 | 4.8 [1.14] |
| 4 | | **4** | 1.0 | 0 | 640 | 0 | 640 | 0 | 100 | 7.2 [1.13] |
| 5 | PA | **1** | 5.7 | 70 | 70 | 13 | 0 | 100 | 0 | 1.3 [1.19] |
| 6 | | **2** | 1.0 | 62 | 180 | 62 | 118 | 34 | 64 | 2.3 [1.14] |
| 7 | | **3** | 0.5 | 52 | 52 | 104 | 0 | 100 | 0 | 3.2 [1.11] |
| 8 | | **4** | 1.0 | 95 | 530 | 95 | 435 | 18 | 82 | 5.3 [1.09] |
| 9[e] | | **4** | 0.6 | 30 | 1440 | 50 | 2350 | 2 | 98 | 5.4 [1.25] |

[a] Polymerization conditions: [cat] : [CHD] : [AH] : [CHO] = 1 : 10 : 100 : 2000, 100 °C, 1 bar $CO_2$. [b] Turnover number (TON), number of moles of AH or CHO consumed/number of moles of catalyst. Moles consumed determined from the $^1$H NMR spectrum by comparing normalized integrals for polycarbonate (4.6 ppm), CHO (3.12 ppm), TCA (5.78 ppm), PA (7.90 ppm), PE (5.70–5.80 and 4.6 ppm) and PE′ (7.50 and 5.14 ppm) resonances. (Fig. S26 and S27). [c] Determined by GPC, in THF, calibrated with narrow molar mass polystyrene standards. (Fig. S28–S36). [d] Turnover frequency (TOF), TON/time (h). [e] [cat] : [CHD] : [AH] : [CHO] = 1 : 10 : 100 : 6000 20 bar $CO_2$.

copolymer structure (rather than mixtures of different polymers) (Fig. S23†).

The most active catalyst, Mg(II)Co(II), shows a significant but slower rate for PA *vs.* carbon dioxide insertion at 1 bar pressure. It was envisaged that at a higher $CO_2$ pressure (20 bar) the rate of carbon dioxide insertion might be biased to favour polycarbonate formation. The polymerization of CHO and PA under 20 bar $CO_2$ resulted in nearly quantitative selectivity for PCHC, as confirmed using *in situ* IR spectroscopy (Fig. S24†). The resulting polymer comprises 98% carbonate and just 2% ester linkages (Fig. S25†). Releasing the carbon dioxide pressure (to <1 bar) after 35 min of reaction, resulted in anhydride consumption and formed a second random copolymer block, as confirmed by NMR spectroscopy (Fig. S25†). Apparently residual carbon dioxide, likely dissolved in solution, competes with anhydride in these insertion reactions. This finding is consistent with the insertion chemistry being kinetically controlled and with these catalysts being highly active for $CO_2$/epoxide ROCOP, even under <1 bar $CO_2$ pressure.[53]

The benefits of the heterodinuclear catalysts, especially **4**, in terms of rate are also apparent compared to the homodinuclear catalysts. For example, at 1 bar pressure catalyst **4** is 20 times faster for $CO_2$/CHO (TOF ~32 $h^{-1}$ for [**1**] : [CHO] = 1 : 1000, 1 bar $CO_2$, 100 °C)[26] and 7 times more active for PA/CHO ROCOP than the di-zinc catalyst **1** (Table 1, entries 5, 8). Compared with the equivalently selective, di-Mg(II) catalyst **2**, its activity is 6 times higher for $CO_2$/CHO ROCOP (Table 1, entries 2, 4). When applied under optimized conditions, catalyst **4** achieves an impressive activity of 2400 $h^{-1}$ for CHO/$CO_2$ ROCOP and maintains high PA/CHO activity even at higher catalyst dilution (Table 1, entry 9).

### Multiblock carbon dioxide derived polymers

The most active catalyst **4**, Mg(II)Co(II), selects for carbon dioxide insertion even under 1 bar pressure. We reasoned that it might be a useful candidate to make multi-block polymers if the gas atmosphere could be reversibly altered (Scheme 2). Such switching would be an appealing means to control carbonate linkage placement within the polymer but it remains unexplored in this field. A triple stainless-steel manifold was constructed allowing for reactions to be subjected to carbon dioxide, nitrogen or vacuum atmospheres (Fig. S37 and S38† for an illustration). Using this apparatus, reactions were conducted under 1 bar pressure of carbon dioxide or nitrogen and switching between these gases is achieved through vacuum–refill cycles; experiments showed that ~6 such cycles are sufficient to reduce carbon dioxide levels in the reaction flask. It is also noted that provided such cycling occurs at temperatures <100 °C, there is no loss of any monomers (as evidenced through external 'traps' and mass balance experiments). The apparatus was used to polymerize mixtures of TCA, CHO and carbon dioxide, exposed to 12 μmol solutions of **4**, in toluene; toluene was used to balance a rate law dependent upon epoxide concentration (*i.e.* maximise epoxide concentration for highest rates) and the increasing solution viscosity, leading to diffusion limitation to rate, for reactions conducted in neat epoxide at higher polymer molar mass. A ten-fold excess *vs.* catalyst of cyclohexane diol was also added to select for α,ω-hydroxyl-telechelic polymers (Scheme S1†). The reaction was monitored by regular removal of aliquots, always prior to changing the reaction gas. The gas switches were timed to ensure that each block showed a degree of polymerization (*DP*) >6. This quantity was determined previously as the lower bound of confidence in complete block enchainment for multi-block polymer structures, given narrow dispersity molar mass distributions.[54] Overall, in all cases, block polymer formation was confirmed by NMR spectroscopy, gel permeation chromatography (GPC) analysis and *in situ* IR spectroscopy (Fig. S40–S51†). Firstly, the reaction was conducted with just one switch – starting under carbon dioxide and, after 1 h, switching the gas with nitrogen. It was predicted that the catalyst should form an ABA triblock polymer based on the faster carbon dioxide than anhydride insertion chemistry, as mentioned previously (B = PCHC, A = PE; Table 2, entry 1). The reaction was conducted under carbon dioxide for 1.3 hours, at which point aliquot analysis revealed

the selective formation of PCHC, showing a molar mass of 6.7 kg mol$^{-1}$ ($Đ$ = 1.15) (Fig. S40†). The reaction atmosphere gas was changed to $N_2$ and the formation of PE was observed by *in situ* IR spectroscopy, as the intensity of the anhydride band at 1780 cm$^{-1}$ decreased (Fig. S41†). Aliquots analysed by NMR spectroscopy confirmed the finding, as the anhydride's sharp doublet peak at 5.77 ppm turned into a broader signal (5.5–5.9 ppm) (Fig. S42†). The formation of an ABA-block polymer was indicated by NMR spectroscopy since block compositions match theoretical predictions based on monomer consumption, by an increase in the molar mass to 9.1 kg mol$^{-1}$ and by DOSY NMR spectroscopy where a single diffusion coefficient was observed for all signals (Fig. S44†). Next, a BABAB pentablock was targeted by two changes in gas atmosphere – starting under carbon dioxide, switching to nitrogen and then switching back to carbon dioxide (Table 2, entry 2). The reaction was initiated under a $CO_2$ atmosphere and PCHC formation was indicated by *in situ* IR spectroscopy (Fig. S45†) and aliquot analysis (NMR spectroscopy) (Fig. S46†); the polycarbonate had a molar mass of 7.5 kg mol$^{-1}$ (Fig. S47†). The atmosphere was switched to $N_2$ and after 2.3 h the complete consumption of the anhydride was observed as a plateau in the conversion *vs.* time data (IR spectroscopy) (Fig. S45†). The intermediary ABA block polymer showed a molar mass of 9.4 kg mol$^{-1}$ (Fig. S47†). Finally, the atmosphere was switched back to $CO_2$ allowing for polycarbonate block growth and the formation of a BABAB pentablock polymer with molar mass of 14.0 kg mol$^{-1}$ (Fig. S47†).

Lastly, an ABABABA heptablock polymer was prepared by three switches of gas atmosphere and following a similar protocol to that described for the pentablock polymer (Table 2, entry 3). *In situ* ATR-IR spectroscopy confirmed the monomer selectivity at each stage with formation of polycarbonate (1230 cm$^{-1}$) or polyester (1780 cm$^{-1}$), as the atmosphere was changed from carbon dioxide to nitrogen (Fig. 2a). Block polymer formation was also confirmed through NMR spectroscopy of aliquots (Fig. S49†) and GPC, with systematic increases to the polymer molar mass and narrow distributions in all cases (Fig. 2c).

The three new multi-block polymers were also analysed using DSC, with all materials being amorphous and showing only a single glass transition temperature consistent with block miscibility (Fig. 2d, S50 and S51†). The $T_g$ values of the multi-blocks increase with the number of blocks, although this may also correlate with the overall increase to molar mass. The $T_g$ values are also all >100 °C and are consistent with previously reported values for PCHC (115 °C)[55] and PE (118–126 °C).[26,56,57] In general, polymers showing high glass transition temperatures are useful since a limitation of current aliphatic polyesters, produced by cyclic ester ring-opening polymerization, has been the moderate/low $T_g$ which results in undesirable softening within useable temperature ranges.[58]

### Pentablocks from $CO_2$/anhydride/epoxide/lactone

In 2016, a DFT investigation of catalyst **1** predicted that a mixture of 4 monomers, namely phthalic anhydride (PA), carbon dioxide, cyclohexene oxide (CHO), and ε-caprolactone (CL), should form only CBABC-pentablock polymer structures (where A = poly(PA-*alt*-CHO), PE′; B = PCHC and C = polycaprolactone PCL).[35] According to the analysis of both barriers and linkage stabilities, the insertion order, into the zinc alkoxide intermediate, should be: PA > carbon dioxide > caprolactone.[35] In 2018, we reported difficulties in experimentally realising this prediction using a di-zinc catalyst because the PCHC chain end underwent backbiting to form cyclic carbonate faster than it initiated lactone ROP.[48] Using catalyst **1**, it was possible to prepare a pentablock BCACB-pentablock (where A = PE′, B = PCHC, C = poly(ε-decalactone), PDL) by adding carbon dioxide after selective catalysis using anhydride, epoxide and lactone to form a CAC triblock polymer.[48] So far, no other

Table 2 Data for multi-block polymer formation from TCA, CHO and 1 bar $CO_2$ with catalyst **4**[a]

| Entry | Block polymer structure | Reaction gas | Time (h) | TON[e] | | Block polymer composition (%) | | $M_n$[f] (kg mol$^{-1}$) [$Đ$] | $DP$[g] | $T_g$[h] (°C) |
|---|---|---|---|---|---|---|---|---|---|---|
| | | | | TCA | CHO | PE | PCHC | | | |
| 1[b] | ABA | $CO_2$ | 1.3 | 0 | 740 | 0 | 100 | 6.7 [1.15] | 74 | 121 |
| | | $N_2$ | 1.2 | 200 | 940 | 21 | 79 | 9.1 [1.17] | 10 | |
| 2[c] | BABAB | $CO_2$ | 1.0 | 0 | 750 | 0 | 100 | 5.7 [1.13] | 75 | 122 |
| | | $N_2$ | 2.3 | 300 | 1050 | 29 | 71 | 9.4 [1.17] | 15 | |
| | | $CO_2$ | 1.7 | 300 | 1777 | 17 | 83 | 14.0 [1.12] | 37 | |
| 3[d] | ABABABA | $CO_2$ | 1.6 | 0 | 1020 | 0 | 100 | 6.0 [1.14] | 102 | 130 |
| | | $N_2$ | 2.2 | 360 | 1380 | 26 | 74 | 11.1 [1.11] | 18 | |
| | | $CO_2$ | 1.7 | 360 | 2520 | 14 | 82 | 17.4 [1.09] | 57 | |
| | | $N_2$ | 4.5 | 600 | 2700 | 20 | 80 | 19.4 [1.07] | 12 | |

[a] All entries run at 100 °C at 1 bar pressure of $CO_2$, 4 M CHO in Toluene. [b] [cat] : [CHD] : [TCA] : [CHO] = 1 : 10 : 200 : 2000. [c] [cat] : [CHD] : [TCA] : [CHO] = 1 : 10 : 300 : 3000. [d] [cat] : [CHD] : [TCA] : [CHO] = 1 : 10 : 600 : 6000. [e] Turnover number (TON), number of moles of TCA or CHO consumed/number of moles of catalyst. Moles consumed determined from the $^1$H NMR spectrum by comparing normalized integrals for PCHC (4.6 ppm), CHO (3.12 ppm), TCA (5.75 ppm) and PE (5.68 ppm) resonances. [f] Determined by GPC, in THF, calibrated with narrow molar mass polystyrene standards. [g] Determined from TON/number of growing chains (initiated by CHD only). [h] Value for multi-block polymer determined by DSC, at 20 °C min$^{-1}$ heating rate, and taken from the second heating/cooling cycle.

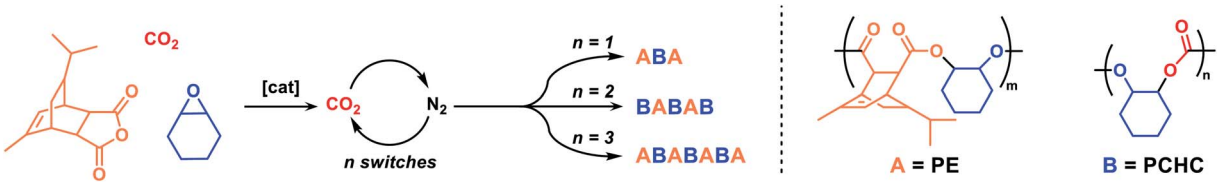


Scheme 2 Multi-block polymer production using catalyst **4** with mixtures of TCA, CHO, and $CO_2$.

catalysts have been shown to selectively enchain from the mixture of these four monomers. We posited that using catalyst **4**, which has distinctive carbon dioxide/anhydride selectivity, should access other pentablock polymers and, in particular, allow production of CABAC patterns. Such an enchainment is predicted since PCHC formation occurs before PE from mixtures and by installing PE end-groups the undesirable PCHC back-biting reactions might be obviated allowing for initiation of lactone ROP, once the carbon dioxide is removed.

Catalyst **4** was added to a solution of TCA (100 equiv.), ε-decalactone (DL, 100 equiv.), CHO (~2000 equiv.), CHD (10 equiv.) and 1 bar pressure of $CO_2$, at 100 °C. The catalysis proceeded with first formation of PCHC (polycarbonate) followed, after switching carbon dioxide for nitrogen gas, by formation of the PE block (TCA/CHO ROCOP). Once the anhydride was consumed, the reaction stopped and no polymerization of DL was observed, even after 8 hours with heating. Aliquot analysis at this point, by $^1$H NMR spectroscopy, confirmed formation of a BAB polymer (B = PE, A = PCHC) but also showed new low intensity signals at 4.93 ppm attributed to cyclohexene carbonate (~1%) (Fig. S52†). The formation of cyclic carbonate is curious since it was absent from aliquots removed prior to complete anhydride consumption. Thus, it seems that the formation of cyclic carbonate is not a result of PCHC block degradation and consistent with this notion, there was no change to the polymer molar mass or dispersity values after failure to initiate DL ROP, as indicated by GPC. Rather, it is proposed that the cyclic carbonate forms from low levels of

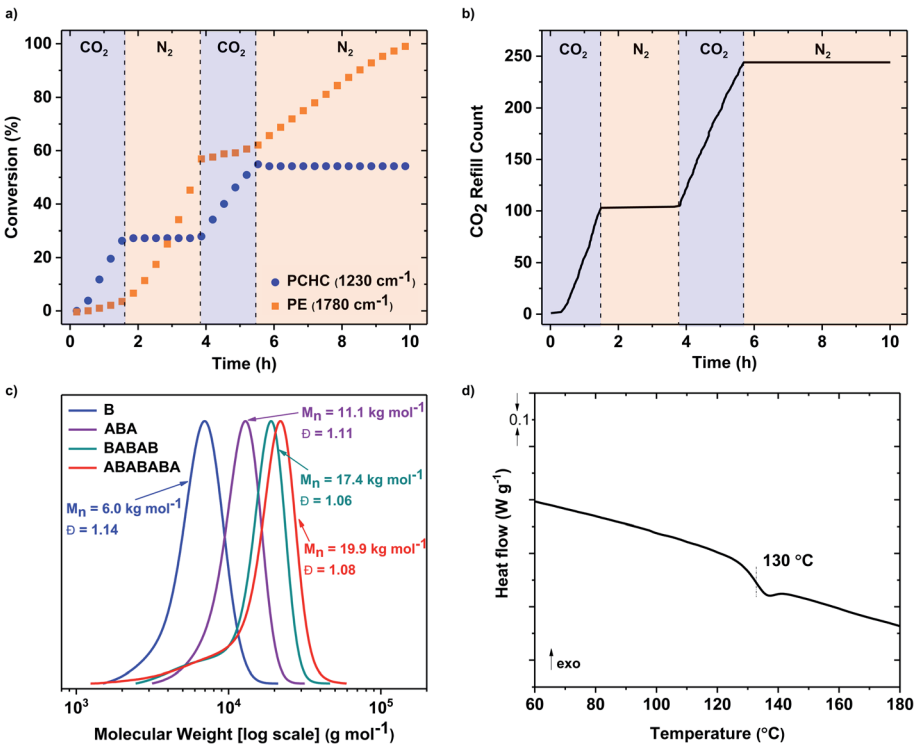


Fig. 2 Data supporting the selective catalysis to form an ABABABA heptablock polymer. Polymerisation conditions **4**: CHD : TCA : CHO 1 : 10 : 600 : 6000, 1 bar $CO_2$, 100 °C, 4 M CHO in toluene. (a) *In situ* IR spectroscopy data are used to construct a plot of conversion *vs.* time showing selective formation of polycarbonate and polyester blocks. (b) The mass-flow controller output is used to determine the frequency of $CO_2$ refill into the reaction vessel, corresponding to the consumption of $CO_2$, as in (a). (c) Analysis of reaction aliquots using GPC, shows a continual evolution of molar mass after each block is formed with narrow dispersity distributions (note that at higher block configurations there is some low molar mass 'tailing' to data which may arise either from contamination by acetate initiated chains and/or from slower initiation from polymeric cyclohexanol end-capped chains). (d) DSC data for the heptablock polymer, determined at 20 °C min$^{-1}$ heating rate, and taken from the second heating/cooling cycle.

dissolved carbon dioxide, perhaps in equilibrium with vapour phases, which preferentially inserts into the PE block zinc alkoxide chain end-group. Such a finding would be consistent with the decomposition of PCHC end-groups to cyclic carbonate and failure to initiate DL ROP.[48] To investigate this phenomenon, a mixture of **4**, TCA, DL and CHO, heated to 100 °C, resulted in the formation of a triblock polymer of the form CAC (C = PDL, A = PE); aliquot analysis confirmed the formation of PE, followed by PDL blocks (Fig. S53 and S54†). This experiment confirms the feasibility of PE end-group initiation of DL ROP. It seems that the polymer end-group sterics/rigidity are not limiting pentablock formation. Accordingly, even low levels of contaminating carbon dioxide appear to result in preferential insertion into metal alkoxide intermediates and trigger a side-reaction in which the carbonate decomposes slowly over time to form cyclic carbonate. To investigate the importance of the relative rate of lactone initiation on pentablock formation, polymerizations using CL in place of DL were undertaken since CL propagates by a primary alkoxide (whereas DL propagates with a secondary alkoxide) (Fig. S55†). Further, there is already precedent for switch catalysis using mixtures of CHO, $CO_2$ and CL to form block polymers.[59] A mixture of **4**, TCA (100 equiv.), CL (200 equiv.), CHO (~2000 equiv.) and 1 bar pressure $CO_2$, heated to 100 °C was polymerized, with the carbon dioxide being exchanged for nitrogen after 0.5 h (Fig. 3a). The catalyst selectively formed the target CABAC-pentablock polymer (where A = PE; B = PCHC and C = PCL) (Table 3). First, the polycarbonate PCHC forms consistent with the catalyst's fast carbon dioxide insertion and was confirmed by NMR spectroscopy where only resonances due to polycarbonate and the unreacted other monomers were observed (Fig. 3c). At this point, the carbon dioxide was switched for nitrogen and TCA/CHO ROCOP occurred. An aliquot removed after 2 hours, shows the growth of the polyester block and GPC analysis shows an increase in molar mass to 5.2 kg mol$^{-1}$ (Fig. 3b). Once all the anhydride was converted, CL ROP occurred. GPC analysis of the aliquots demonstrate an increase in molar mass consistent with block polymer formation (Fig. 3b). The final aliquot, after PCL growth, shows a broader dispersity attributed to slower rates of initiation (from a secondary cyclohexanol group) *vs.* propagation (from a primary hydroxyl group) during CL ROP.[60] The final pentablock polymer was analysed by DSC and showed a single $T_g$ value of 86 °C, indicative of block miscibility and demonstrating the utility in incorporating 'softer' aliphatic polyesters (Fig. S59†).

## Discussion

These polymerizations show that carbon dioxide insertion rates, are strongly metal dependent. Even though such rates are difficult to directly measure as they occur in the pre-rate limiting step in catalysis ($k_2$ and $k_3$ in Fig. 4a), they can be inferred from the monomer selectivity from mixtures. Given that other $CO_2$/epoxide ROCOP catalysts also show zeroth order rate dependencies on carbon dioxide pressure, the findings are likely more broadly significant.[19,61–64] Accordingly, for this series of catalysts the carbon dioxide insertion rates follow the trend Co(II) > Mg(II) > Zn(II). In these polymerizations, where selectivity occurs through competition between anhydride and carbon dioxide, catalysts featuring Mg(II) are selective for $CO_2$ insertion, whereas the di-Zn(II) analogues are selective for anhydride insertion. Most other catalysts in this field are also highly selective for anhydride insertion.[6,14,22,23,27,65,66] There are very few other examples of catalysts selective for carbon dioxide over anhydride.[20,25,46] This year, Feng and co-workers reported specific conditions under which a triethyl borane and bis(triphenylphosphine)iminium chloride (PPNCl) catalyst system (**I**) formed random copolymers from mixtures of PA/CHO/$CO_2$ (Fig. 4b).[46] These reactions required 10 bar $CO_2$ pressure and only yielded the randomized enchainment at ratios of PPNCl : $Et_3B$ : PA : CHO in the range 1 : 3 : 50–80 : 200, *i.e.* at very high loading of catalyst relative to PA.[46] At lower catalyst loadings/higher PA proportion, the catalysts were deactivated. A further issue is that the polymers all show bimodal molar mass distributions which would preclude any selective block or multiblock formation. Finally, it should be noted that the organocatalytic system must be very finely balanced since Lu and co-workers showed that the same catalyst system exposed to the same monomer ratios but at 1 bar $CO_2$ pressure formed the expected poly(ester-*b*-carbonate) – *i.e.* anhydride insertion was selected.[27] Another limitation of this organocatalyst system is its modest activity ($TOF_{CHO/PA}$ = 5 h$^{-1}$, $TOF_{CHO/CO2}$ = 3.5 h$^{-1}$, PPNCl : $Et_3B$ : PA : CHO : $CO_2$, 1 : 3 : 80 : 200, 16 h, 10 bar, 80 °C). In comparison catalyst **4** shows higher activity ($TOF_{CHO/PA}$ = 95 h$^{-1}$, $TOF_{CHO/CO2}$ = 460 h$^{-1}$, **4** : [CHD] : [AH] : [CHO] = 1 : 10 : 100 : 2000, 100 °C, 1 bar $CO_2$, Table 1, entry 8). Coates and co-workers found that at $CO_2$ pressures >27 bar, the Zn(II) catalyst (**II**) randomly inserted $CO_2$ into the DGA/CHO polyester.[20]

In terms of future directions for these dinuclear catalysts, other catalysts containing Group 1 or 2 metals should be explored to understand whether they also show beneficial influences over carbon dioxide insertion chemistry. Recently highly active heterodinuclear Co(III)M(I) (M = Na, K) catalysts for carbon dioxide/epoxide ROCOP were reported and these species should also be explored in switchable catalysis.[63,67] The findings also underscore the central importance of the metal selection in dictating both the polymerization activity (rate determining step) and selectivity (pre-rate limiting step). In particular, inexpensive and light Mg(II)-based catalysts appear to be beneficial in selecting for carbon dioxide placement over anhydride in more complex polymer structures.

This work demonstrates a straightforward method to make multi-block polymers. Until now, such structures were not investigated and any preparations would have required several sequential monomer additions; such processes can be difficult to control, time correctly and may also introduce impurities which compromise molar mass distributions. In contrast, here the best Mg(II)Co(II) catalyst yields, by simple gas environment switches, tri-, penta- and heptablock structures. This work also demonstrates its potential to sequentially access three different polymerization pathways: epoxide/anhydride ROCOP, carbon dioxide/epoxide ROCOP and lactone ROP. There is just one prior report of a di-Zn(II) catalyst able to enchain selectively

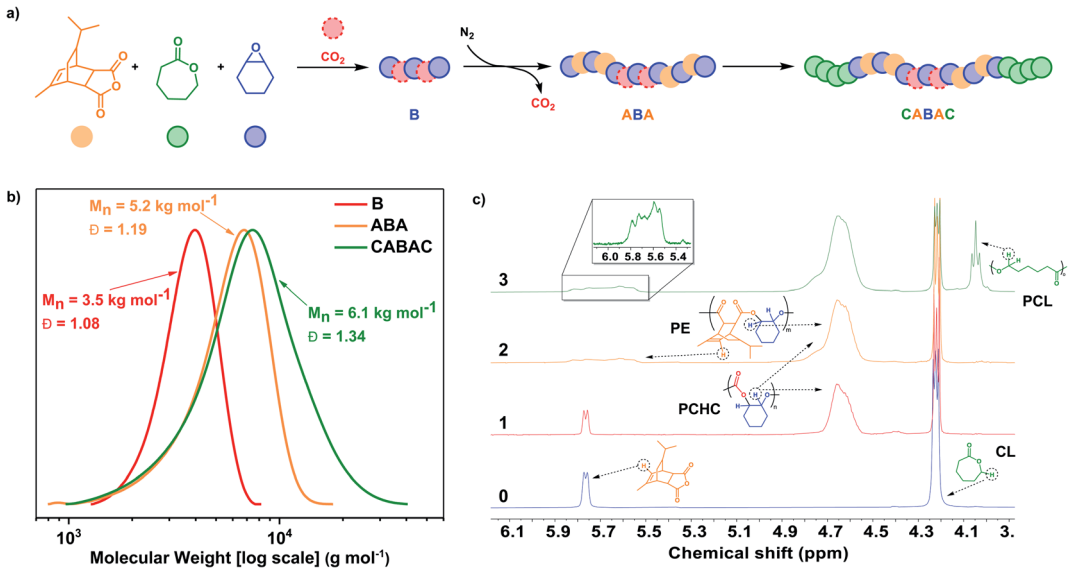


Fig. 3 Selective polymerization catalysis using **4** and mixtures of TCA (orange), CL (green), CHO (blue), and carbon dioxide (red). Polymerization conditions: [**4**] : [CHD] : [TCA] : [CL] : [CHO] = 1 : 10 : 100 : 200 : 2000, 1 bar $CO_2$, 100 °C (a) illustration of the block polymer structure and simplified representation using coloured 'balls' to represent different monomers. (b) GPC analysis of aliquots removed at different times (corresponding to entries 1, 2, and 3 in Table 3) during the reaction and showing the formation of PCHC, PE-PCHC-PE and PCL-PE-PCHC-PE-PCL. (c) Stack plot showing a selected region of the $^1$H NMR spectra of aliquots removed during formation of the polymer blocks. Spectrum 0 is the mixture before polymerization. The first block that formed is PCHC, shown by the resonance at 4.6 ppm, the second is PE, shown by the loss of the sharp doublet into a broad polymer signal at 5.8 ppm, and the final PCL block in 3 from the new signal at 4.0 ppm. For complete spectra see Fig. S56.†

from these four monomers.[48] In comparison, **4** yields both a new multi-block structure and accelerates the rate by 10 fold for CHO/$CO_2$ ROCOP and 3 fold for the AH/CHO ROCOP ($TOF_{PCHC} = 650\ h^{-1}$ for **4** *vs.* 6 $h^{-1}$ for **1**; $TOF_{PE} = 67\ h^{-1}$ for **4** *vs.* 27 $h^{-1}$ for **1**).[48]

Here, the focus has been on improving the catalytic selectivity, activity and in making new multi-block structures. These catalytic discoveries should be generalizable to a wide range of new structures and property investigation is warranted. Controlling the block sequence is obviously a means to moderate the polymer's glass transition temperature and end-group chemistry. Here, such selectivity relies upon the dinuclear catalysts being applied with excess (>10 equiv. *vs.* catalyst) of a chain transfer agent, such as cyclohexane diol, and the resulting polymers are low molar mass hydroxyl-telechelic, *i.e.* polyols.[3] Such polyols could be useful to make higher polymers like polyurethanes, cross-linked resins or as surfactants.[13,68,69] The new structures accessible using these catalysts should prove valuable in furthering understanding of how polymer composition and sequence influence the polyol rheology, viscosity, reactivity through end-group chemistry, thermal stability and degradation chemistry.[4] It is now well-established that alkene-functionalized monomers, including vinylcyclohexene oxide, can be efficiently and quantitatively post-functionalized to install carboxylic acid, hydroxyl, amine and sulfonate functional groups to the polymer backbone.[36,70–76] In future, combining these selective catalyses with post-functionalizations could deliver new surfactants, self-assembled nanostructures, colloids and electrolytes without needing to increase polymer molar mass.[72,73] An important target for future study are catalysts featuring organometallic initiators since these species allow for reduced loading of chain

Table 3 Data for the formation of a pentablock polymer from TCA, CHO, CL and $CO_2$ using catalyst **4**[a]

| Entry | Reaction gas | Time (h) | TON[b] TCA | CL | CHO | TOF ($h^{-1}$)[c] | $M_n$ (kg $mol^{-1}$) [$Đ$][d] |
|---|---|---|---|---|---|---|---|
| 1 | $CO_2$ | 0.5 | 0 | 0 | 325 | 650 | 3.5 [1.08] |
| 2 | $N_2$ | 1.5 | 100 | 0 | 425 | 67 | 5.2 [1.19] |
| 3 | $N_2$ | 3.0 | 100 | 86 | 460 | 29 | 6.1 [1.34] |

[a] [cat] : [CHD] : [TCA] : [CL] : [CHO] = 1 : 10 : 100 : 200 : 2000, 100 °C, entry 1 under 1 bar of $CO_2$ for 0.5 h, Entry 2 under 1 bar of $N_2$ for 1.5 h and 3 for 3.0 h. [b] Turnover number (TON), number of moles of TCA or CHO consumed/number of moles of catalyst. Moles consumed determined by $^1$H NMR, by comparison of the relative integrals of the resonances due to monomer (TCA 5.73 ppm, CHO 3.08 ppm, CL 4.18 ppm) and polymer (PE 4.63 ppm, PCHC 4.63 ppm, PCL 4.02 ppm) (Fig. S56). [c] Turnover frequency (TOF), TON/time (h). [d] Measured by GPC, in THF, using narrow MW polystyrene standards to calibrate the instrument.

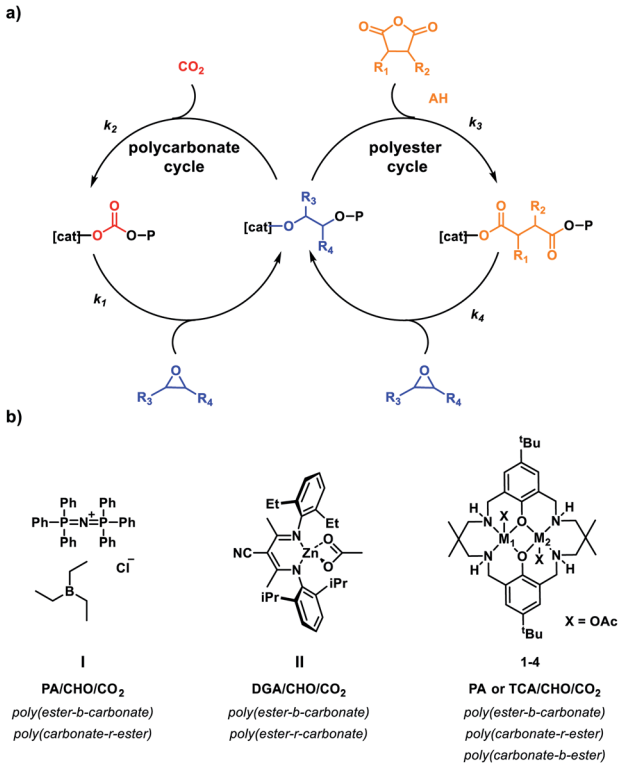


Fig. 4 (a) Catalytic cycles for carbon dioxide/epoxide and anhydride/epoxide ROCOP which are accessed by the catalysts to build up block polymers. (b) Catalysts which exhibit unexpected selectivity for carbon dioxide *vs.* anhydride ($k_2 > k_3$) depending on reaction conditions (pressure, concentration, monomer, metal centre).

transfer agent and access higher molar mass polymers.[38] Such materials would be expected to undergo phase separation and there is emerging evidence that multi-block polymers may afford new nanostructures and improve upon thermal mechanical properties compared with equivalent di- or triblock structures.[47,77,78]

## Conclusions

Highly active and selective switchable polymerization catalysts form multi-block polymers featuring ester and carbonate linkages, with predictable and controlled placement of both the monomers and the blocks in the overall polymer structure. The catalysts, coordinated by a macrocyclic ancillary ligand, feature both homo- and heterodinuclear combinations of metals [Mg(II) Mg(II), Zn(II)Zn(II), Zn(II)Mg(II) and Mg(II)Co(II)]. Catalysts featuring Mg(II) show a strong preference for carbon dioxide *vs.* anhydride insertion – an unusual finding since almost all other catalysts in this field show the inverse selectivity. Further, the Mg(II)Co(II) catalyst combines very high carbon dioxide selectivity with outstanding rates across both polymerization cycles, allowing for up to 20 fold improvement in activity compared to di-Mg(II) or di-Zn(II) catalysts. The Mg(II)Co(II) catalyst was used to make tri-, penta- and heptablock sequences from mixtures of carbon dioxide, anhydride (tricyclic anhydride, a bio-based monomer) and cyclohexene oxide. It also enchains selectively a four-component mixture (cyclohexene oxide, tricyclic anhydride, carbon dioxide and caprolactone) to make a single sequenced pentablock polymer. These results demonstrate the importance of continued focus on both catalytic activity and selectivity. They may also be significant in polymer materials contexts since by controlling the monomer mixture composition, it is feasible to control the end-group chemistry and glass transition temperature for the resulting polymers. With routes to control sequence in these polymers, in future their polymer chemistry, rheology, degradation chemistry and functional substituents should be investigated. Finally, it is noted that by using carbon dioxide and bio-derived anhydrides it is possible to increase the renewable content in these polymers which may offer benefits in terms of reduced greenhouse gas emissions and sustainability.

## Data availability

All experimental procedures, charactarisation, and NMR spectra for polymerizations can be found in the ESI.†

## Author contributions

GR conducted all experimental work, ACD and CKW supervised the research and all authors wrote the manuscript. CKW secured all research funding and leads the research group.

## Conflicts of interest

CKW is a director of econic technologies.

## Acknowledgements

The EPSRC (EP/S018603/1; EP/R027129/1), Oxford Martin School (Future of Plastics Programme) and SCG Chemicals (Studentship to GR) are acknowledged for research funding.

## References

1 C. Hepburn, E. Adlen, J. Beddington, E. A. Carter, S. Fuss, N. Mac Dowell, J. C. Minx, P. Smith and C. K. Williams, *Nature*, 2019, **575**, 87–97.
2 J. Artz, T. E. Müller, K. Thenert, J. Kleinekorte, R. Meys, A. Sternberg, A. Bardow and W. Leitner, *Chem. Rev.*, 2018, **118**, 434–504.
3 D. J. Darensbourg, *Green Chem.*, 2019, **21**, 2214–2223.
4 M. Scharfenberg, J. Hilf and H. Frey, *Adv. Funct. Mater.*, 2018, **28**, 1704302.
5 B. Grignard, S. Gennen, C. Jérôme, A. W. Kleij and C. Detrembleur, *Chem. Soc. Rev.*, 2019, **48**, 4466–4514.
6 J. M. Longo, M. J. Sanford and G. W. Coates, *Chem. Rev.*, 2016, **116**, 15167–15197.
7 Y.-Y. Zhang, G.-P. Wu and D. J. Darensbourg, *Trends Chem.*, 2020, **2**, 750–763.
8 A. C. Deacy, G. L. Gregory, G. S. Sulley, T. T. D. Chen and C. K. Williams, *J. Am. Chem. Soc.*, 2021, **143**, 10021–10040.

9 C. Diaz and P. Mehrkhodavandi, *Polym. Chem.*, 2021, **12**, 783–806.
10 G. X. De Hoe, M. T. Zumstein, B. J. Tiegs, J. P. Brutman, K. McNeill, M. Sander, G. W. Coates and M. A. Hillmyer, *J. Am. Chem. Soc.*, 2018, **140**, 963–973.
11 M. J. Sanford, N. J. Van Zee and G. W. Coates, *Chem. Sci.*, 2018, **9**, 134–142.
12 N. Yi, T. T. D. Chen, J. Unruangsri, Y. Zhu and C. K. Williams, *Chem. Sci.*, 2019, **10**, 9974–9980.
13 G.-W. Yang and G.-P. Wu, *ACS Sustainable Chem. Eng.*, 2019, **7**, 1372–1380.
14 S. Ye, W. Wang, J. Liang, S. Wang, M. Xiao and Y. Meng, *ACS Sustainable Chem. Eng.*, 2020, **8**, 17860–17867.
15 N. Zhu, X. Hu, Z. Fang and K. Guo, *Prog. Polym. Sci.*, 2021, **117**, 101397.
16 D. J. Darensbourg, *Inorg. Chem. Front.*, 2017, **4**, 412–419.
17 X. Zhang, M. Fevre, G. O. Jones and R. M. Waymouth, *Chem. Rev.*, 2018, **118**, 839–885.
18 S. Paul, Y. Zhu, C. Romain, R. Brooks, P. K. Saini and C. K. Williams, *Chem. Commun.*, 2015, **51**, 6459–6479.
19 J. Liang, S. Ye, S. Wang, M. Xiao and Y. Meng, *Polym. J.*, 2021, **53**, 3–27.
20 R. C. Jeske, J. M. Rowley and G. W. Coates, *Angew. Chem., Int. Ed.*, 2008, **47**, 6041–6044.
21 C. E. Koning, R. J. Sablong, E. H. Nejad, R. Duchateau and P. Buijsen, *Prog. Org. Coat.*, 2013, **76**, 1704–1711.
22 S. Huijser, E. HosseiniNejad, R. Sablong, C. de Jong, C. E. Koning and R. Duchateau, *Macromolecules*, 2011, **44**, 1132–1139.
23 D. J. Darensbourg, R. R. Poland and C. Escobedo, *Macromolecules*, 2012, **45**, 2242–2248.
24 J. Y. Jeon, S. C. Eo, J. K. Varghese and B. Y. Lee, *Beilstein J. Org. Chem.*, 2014, **10**, 1787–1795.
25 P. K. Saini, C. Romain, Y. Zhu and C. K. Williams, *Polym. Chem.*, 2014, **5**, 6068–6075.
26 P. K. Saini, G. Fiorani, R. T. Mathers and C. K. Williams, *Chem. - Eur. J.*, 2017, **23**, 4260–4265.
27 J. Zhang, L. Wang, S. Liu, X. Kang and Z. Li, *Macromolecules*, 2021, **54**, 763–772.
28 A. J. Plajer and C. K. Williams, *Angew. Chem., Int. Ed.*, 2021, DOI: 10.1002/anie.202104495.
29 Y. Liu, K. Deng, S. Wang, M. Xiao, D. Han and Y. Meng, *Polym. Chem.*, 2015, **6**, 2076–2083.
30 Y. Liu, K. Huang, D. Peng and H. Wu, *Polymer*, 2006, **47**, 8453–8461.
31 Y. Liu, M. Xiao, S. Wang, L. Xia, D. Hang, G. Cui and Y. Meng, *RSC Adv.*, 2014, **4**, 9503–9508.
32 C. Romain and C. K. Williams, *Angew. Chem., Int. Ed.*, 2014, **53**, 1607–1610.
33 T. Stößer, T. T. D. Chen, Y. Zhu and C. K. Williams, *Philos. Trans. R. Soc., A*, 2018, **376**, 20170066.
34 Y. Zhu, C. Romain and C. K. Williams, *J. Am. Chem. Soc.*, 2015, **137**, 12179–12182.
35 C. Romain, Y. Zhu, P. Dingwall, S. Paul, H. S. Rzepa, A. Buchard and C. K. Williams, *J. Am. Chem. Soc.*, 2016, **138**, 4120–4131.
36 T. Stößer, G. S. Sulley, G. L. Gregory and C. K. Williams, *Nat. Commun.*, 2019, **10**, 2668.
37 S. Kernbichl, M. Reiter, J. Mock and B. Rieger, *Macromolecules*, 2019, **52**, 8476–8483.
38 G. S. Sulley, G. L. Gregory, T. T. D. Chen, L. Peña Carrodeguas, G. Trott, A. Santmarti, K.-Y. Lee, N. J. Terrill and C. K. Williams, *J. Am. Chem. Soc.*, 2020, **142**, 4367–4378.
39 S. Zhu, Y. Zhao, M. Ni, J. Xu, X. Zhou, Y. Liao, Y. Wang and X. Xie, *ACS Macro Lett.*, 2020, **9**, 204–209.
40 W. T. Diment, T. Stößer, R. W. F. Kerr, A. Phanopoulos, C. B. Durr and C. K. Williams, *Catal. Sci. Technol.*, 2021, **11**, 1737–1745.
41 T. Stößer and C. K. Williams, *Angew. Chem., Int. Ed.*, 2018, **57**, 6337–6341.
42 T. Stößer, D. Mulryan and C. K. Williams, *Angew. Chem., Int. Ed.*, 2018, **57**, 16893–16897.
43 A. Virachotikul, N. Laiwattanapaisarn, P. Wongmahasirikun, P. Piromjitpong, K. Chainok and K. Phomphrai, *Inorg. Chem.*, 2020, **59**, 8983–8994.
44 W.-B. Li, Y. Liu and X.-B. Lu, *Organometallics*, 2020, **39**, 1628–1633.
45 F. de la Cruz-Martínez, M. Martínez de Sarasa Buchaca, J. Martínez, J. Tejeda, J. Fernández-Baeza, C. Alonso-Moreno, A. M. Rodríguez, J. A. Castro-Osma and A. Lara-Sánchez, *Inorg. Chem.*, 2020, **59**, 8412–8423.
46 V. K. Chidara, S. K. Boopathi, N. Hadjichristidis, Y. Gnanou and X. Feng, *Macromolecules*, 2021, **54**, 2711–2719.
47 Y. Li, Y.-Y. Zhang, L.-F. Hu, X.-H. Zhang, B.-Y. Du and J.-T. Xu, *Prog. Polym. Sci.*, 2018, **82**, 120–157.
48 T. T. D. Chen, Y. Zhu and C. K. Williams, *Macromolecules*, 2018, **51**, 5346–5351.
49 D. Dakshinamoorthy, A. K. Weinstock, K. Damodaran, D. F. Iwig and R. T. Mathers, *ChemSusChem*, 2014, **7**, 2923–2929.
50 N. J. Van Zee, M. J. Sanford and G. W. Coates, *J. Am. Chem. Soc.*, 2016, **138**, 2755–2761.
51 J. A. Garden, P. K. Saini and C. K. Williams, *J. Am. Chem. Soc.*, 2015, **137**, 15078–15081.
52 A. C. Deacy, A. F. R. Kilpatrick, A. Regoutz and C. K. Williams, *Nat. Chem.*, 2020, **12**, 372–380.
53 S. K. Raman, R. Raja, P. L. Arnold, M. G. Davidson and C. K. Williams, *Chem. Commun.*, 2019, **55**, 7315–7318.
54 G. Gody, P. B. Zetterlund, S. Perrier and S. Harrisson, *Nat. Commun.*, 2016, **7**, 10514.
55 C. Koning, J. Wildeson, R. Parton, B. Plum, P. Steeman and D. J. Darensbourg, *Polymer*, 2001, **42**, 3995–4004.
56 N. J. Van Zee and G. W. Coates, *Angew. Chem., Int. Ed.*, 2015, **54**, 2665–2668.
57 M. J. Sanford, L. Peña Carrodeguas, N. J. Van Zee, A. W. Kleij and G. W. Coates, *Macromolecules*, 2016, **49**, 6394–6400.
58 D. K. Schneiderman and M. A. Hillmyer, *Macromolecules*, 2016, **49**, 2419–2428.
59 S. Paul, C. Romain, J. Shaw and C. K. Williams, *Macromolecules*, 2015, **48**, 6047–6056.
60 Y. Zhu, C. Romain, V. Poirier and C. K. Williams, *Macromolecules*, 2015, **48**, 2407–2416.

61 C. M. Kozak, K. Ambrose and T. S. Anderson, *Coord. Chem. Rev.*, 2018, **376**, 565–587.
62 J. Deng, M. Ratanasak, Y. Sako, H. Tokuda, C. Maeda, J.-y. Hasegawa, K. Nozaki and T. Ema, *Chem. Sci.*, 2020, **11**, 5669–5675.
63 W. Lindeboom, D. A. X. Fraser, C. B. Durr and C. K. Williams, *Chem.–Eur. J.*, 2021, **27**(47), 12224–12231.
64 D. R. Moore, M. Cheng, E. B. Lobkovsky and G. W. Coates, *J. Am. Chem. Soc.*, 2003, **125**, 11911–11924.
65 C.-H. Chang, C.-Y. Tsai, W.-J. Lin, Y.-C. Su, H.-J. Chuang, W.-L. Liu, C.-T. Chen, C.-K. Chen and B.-T. Ko, *Polymer*, 2018, **141**, 1–11.
66 S. Pappuru and D. Chakraborty, *Eur. Polym. J.*, 2019, **121**, 109276.
67 A. C. Deacy, E. Moreby, A. Phanopoulos and C. K. Williams, *J. Am. Chem. Soc.*, 2020, **142**, 19150–19160.
68 N. von der Assen and A. Bardow, *Green Chem.*, 2014, **16**, 3272–3280.
69 D. J. Darensbourg and F.-T. Tsai, *Macromolecules*, 2014, **47**, 3806–3813.
70 G.-W. Yang, Y.-Y. Zhang, Y. Wang, G.-P. Wu, Z.-K. Xu and D. J. Darensbourg, *Macromolecules*, 2018, **51**, 1308–1313.
71 B. Han, B. Liu, H. Ding, Z. Duan, X. Wang and P. Theato, *Macromolecules*, 2017, **50**, 9207–9215.
72 T. Stößer, C. Li, J. Unruangsri, P. K. Saini, R. J. Sablong, M. A. R. Meier, C. K. Williams and C. Koning, *Polym. Chem.*, 2017, **8**, 6099–6105.
73 K. Deng, S. Wang, S. Ren, D. Han, M. Xiao and Y. Meng, *ACS Appl. Mater. Interfaces*, 2016, **8**, 33642–33648.
74 D. J. Darensbourg and Y. Wang, *Polym. Chem.*, 2015, **6**, 1768–1776.
75 D. J. Darensbourg, W.-C. Chung, C. J. Arp, F.-T. Tsai and S. J. Kyran, *Macromolecules*, 2014, **47**, 7347–7353.
76 J. Geschwind, F. Wurm and H. Frey, *Macromol. Chem. Phys.*, 2013, **214**, 892–901.
77 I. Lee, T. R. Panthani and F. S. Bates, *Macromolecules*, 2013, **46**, 7387–7398.
78 E. Grune, M. Appold, A. H. E. Müller, M. Gallei and H. Frey, *ACS Macro Lett.*, 2018, **7**, 807–810.